scientific reports

Check for updates

OPEN

Effect of heat and mass transfer on the nanofluid of peristaltic flow in a ciliated tube

A. M. Abd-Alla[1], S. M. Abo-Dahab[2], M. A. Abdelhafez[1] & Y. Elmhedy[1]✉

The current work focuses attention on discussing the peristaltic flow of Rabinowitsch nanofluid through ciliated tube. This technical study analyzes heat and mass transfer effects on the flow of a peristaltic flow, incompressible, nanofluid via a ciliated tube. The governing non-linear partial differential equations representing the flow model are transmuted into linear ones by employing the appropriate non-dimensional parameters under the assumption of long wavelength and low Reynolds number. The flow is examined in wave frame of reference moving with the velocity *c*. The governing equations have been solved to determine velocity, temperature, concentration, the pressure gradient, pressure rise and the friction force. Using MATLAB R2023a software, a parametric analysis is performed, and the resulting data is represented graphically. The results indicate that the various emerging parameters of interest significantly affect the nanofluid properties within the tube. The present study enhances the comprehension of nanofluid dynamics in tube and offers valuable insights into the influence of heat and mass transfer in such setups. Convective heat transfer is found to be greater at the boundaries resulting in decreased temperature there.

List of symbols

c	Wave speed
C	Concertation
$\left(\frac{dp}{dx}\right)$	Pressure gradient
(Δp_λ)	Pressure rise
(F_λ)	Friction force and
(S_{rz})	Shear stress
R	Radius
Z	Axis of the tube
Z_0	Reference position of the cilia
k_{nf}	Thermal conductivity of nanofluid
k_f	Thermal conductivity of fluid
Q Q	Heat source
α	Measure of the eccentricity of the elliptic motion of the cilia
α_c	Coefficient of the viscosity at constant concentration
Br	Brinkman number
$(\rho\beta)_{nf}$	Thermal coefficient of nanofluid
β_f	The thermal expansion coefficient
Gr	Grash of number
λ	Wavelength
λ_1	Ratio of relaxation to retardation times
λ_2	Retardation time and dots denote the differentiation with respect to time
ε	Cilia length
$\overline{S}$	Extra stress tensor
Sr	Soret number
Sc	Schmidt number
Re	Reynolds number
Q	Heat source

[1]Mathematics Department, Faculty of Science, Sohag University, Sohag, Egypt. [2]Mathematics Department, Faculty of Science, South Valley University, Qena, Egypt. ✉email: yasmine.elmhedy@gmail.com

Q_O	Heat generation coefficient
g	Gravity constant
δ	Wavenumber
$\overline{\dot{\gamma}}$	Shear rate
$\overline{T}_0$	Temperature of the inner tube
$\overline{U}$ and $\overline{V}$	Velocity components in radial and axial directions
w	Velocity profile of Rabinowitsch nanofluid
a	Radius of the tube
ρ_s, $(\rho\beta)_s$, $(\rho c_p)_s$	Density, the thermal expansion coefficient, the effective heat capacitance
K_s	Thermal conductivity of the solid particle
θ	Temperature

Advances in fluids engineering and industrial sectors have aroused the interest of researchers in analysing mathematical models for non-Newtonian fluids. Non-Newtonian materials include slurries, coolants, lubricants, blood at low shear rates, ketchup, some paints, dirt, hygienic products, and many more. Several researchers have extensively studied the flow characteristics of such fluids due to their critical importance in the diverse fields of science and technology, including polymer solutions, viscoelastic suspensions, metal spinning, lubricants, plastics manufacturing, molten metal distillation, crystals, and food processing. Given its significance, a single constitutive model cannot encompass all non-Newtonian fluid aspects due to the diverse nature of fluid characteristics. The Peristaltic flow is a common method of fluid flow where flexible chambers are used to propel fluids through progressive waves of contraction and expansion. Akbar et al.[1] studied the magnetohydrodynamics and convective heat transfer of nanofluids synthesized by three different shaped (brick, platelet and cylinder) silver nanoparticles in water. Narla et al.[2] investigated the analysis of entropy generation in biomimetic electroosmotic nanofluid pumping through a curved channel with joule dissipation. Agoor et al.[3] examined the binary powell-eyring nanofluid of peristaltic flow with heat transfer in a ciliated tube. Shit and Majee[4] discussed a pulsatile MHD flow of blood signifying blood as a Newtonian fluid with temperature-dependent variable viscosity in an overlapping constricted tube under the influence of whole-body vibration. In a separate study, Shit and Majee[5] examined the unsteady MHD flow of blood and thermal effect in an aneurysmatic artery using a finite difference approach. They documented that with increasing the magnitude of the Prandtl number, the Nusselt number enhances. Thermal radiation therapy is of significant importance in some medical procedures related to the cure of muscle spasm, myalgia (muscle pain), fibromyalgia and contracture. Maqbool et al.[6] studied the effects of magnetic field and copper nanoparticles on the flow of tangent hyperbolic fluid through a ciliated tube. Tariq and Khan[7] explained the behavior of second-grade dusty fluid flowing through a flexible tube whose walls are induced by the peristaltic movement. Ellahi et al.[8] discussed the effects of heat and mass transfer on peristaltic flow in a non-uniform rectangular duct is studied under consideration of long wavelength and low Reynolds number. Nadeem et al.[9] investigated the mathematical model for the peristaltic flow of nanofluid through eccentric tubes comprising porous medium. Shaheen and Nadeem[10] analyzed the mathematical model of ciliary motion in an annulus is studied the effect of convective heat transfer and nanoparticle are taken into account. Iqbal et al.[11] investigates the heat and mass transfer through curved channel with bi-convection. Main findings of the analysis discloses that the temperature of nanofluid decreases as radiation and viscosity varies. Abd-Alla et al.[12] explained the effects of heat transfer and the endoscope on Jeffrey fluid peristaltic flow in tubes. Akhtar et al.[13] construct polynomial scheme to find exact solution to the peristaltic flow of Casson fluid through elliptic duct. They focus their attention on the behavior of streamlines. Consideration of constant density force streamlines to be closed enough so that velocity get increased. Peristaltic flow of micropolar fluid through asymmetric channel with new type of interfacial thin film layer at the boundaries are studied by Mahmood et al.[14]. Tanveer et al.[15] presented the analysis for peristaltic flow of Walter's B fluid with internal heat generation. They applied numerical technique based on shooting method which express results in terms of interpolating function. Mansour and Abou-zeid[16] studied the influence of heat and mass transfer the peristaltic flow of non-Newtonian Williamson fluid in the gap between concentric tubes. Awan et al.[17] explained the numerical treatment for dynamics of second law analysis and magnetic induction effects on ciliary induced peristaltic transport of hybrid nanomaterial. Akbar and Butt[18] investigated the concerns with the mechanical properties of a Rabinowitsch fluid model and the effects of thermal conductivity over it. In recent years, researchers have extensively focused on the peristaltic flow of Newtonian and non-Newtonian fluids (see for example[19–31] and several references therein. In Refs.([34–40]), peristaltic flow with new parameters with or without endoscope has been discussed.

Recently, significant interest has been developed in studying a peristaltic phenomenon due to its significant implications in biological sciences and biomedical engineering. In the current study, an investigation is carried out to inspect the peristaltic pattern of the nanofluid model in the presence of mass and heat phenomenon. The flow modelling is followed with the small Reynolds number hypothesis while the long wavelength is premised. The influence of various emerging physical parameters in the obtained solutions is observed. The obtained expressions are utilized to discuss the role of emerging parameters on the flow quantities. Numerical computations have been used to evaluate the expression for velocity, temperature, concentration, the gradient pressure, rise pressure and the friction force of various interesting parameters. Finally, the effect of various emerging parameters is discussed through graphs. Finally, the detailed computational results are compiled and discussed with the physical interpretation of our results. The graphical upshots for the velocity, temperature, concentration, the gradient pressure, rise pressure and the friction force are examined for influentrial parameters.

Flow description

The current analysis is performed to study the 2-dimensional peristaltic flow of Rabinowitsch nanofluid in an infinite tube with convective boundary condition. In addition, we also analyze the impact of nanofluid, thermal conductivity of fluid, the viscosity at constant concentration, thermal coefficient of nanofluid and heat source. For problem under consideration, geometry is exhibited in cylindrical coordinate system (r, θ, z) representing radial, azimuthal and axial coordinates respectively. Furthermore, the fluid flow is caused by the metachronal wave, resulting from uniform cilia beating whereas the temperature and concentration at the wall are T_0 and C_0 respectively (please, see Fig. 1).

Formulation of the problem

For the peristaltic flow of an incompressible nanofluid with iron oxide nanoparticles in a uniform tube, using the cylindrical coordinate (R, Z) where Z the axis of the tube, while R the radius of it see Fig. 1. The flow is described in two coordinate systems one is fixed and the other, moving with speed c.

The equations of motion for the Rabinowitsch nanofluid model for the flow are[18,32,33]

$$\frac{\partial \overline{U}}{\partial \overline{R}} + \frac{\overline{U}}{\overline{R}} + \frac{\partial \overline{W}}{\partial \overline{Z}} = 0. \tag{1}$$

The r component of momentum equation:

$$\rho_{nf}\left(\frac{\partial \overline{U}}{\partial \overline{t}} + \overline{U}\frac{\partial \overline{U}}{\partial \overline{R}} + \overline{W}\frac{\partial \overline{U}}{\partial \overline{Z}}\right) = -\frac{\partial \overline{P}}{\partial \overline{R}} + \frac{1}{\overline{R}}\frac{\partial}{\partial \overline{R}}\left(\overline{R}\bar{\bar{S}}_{\overline{RR}}\right) + \frac{\partial \bar{\bar{S}}_{\overline{RZ}}}{\partial \overline{Z}} - \frac{\overline{S}_{\overline{\theta\theta}}}{\overline{R}}. \tag{2}$$

The z component of momentum equation:

$$\rho_{nf}\left(\frac{\partial \overline{W}}{\partial \overline{t}} + \overline{U}\frac{\partial \overline{W}}{\partial \overline{R}} + \overline{W}\frac{\partial \overline{W}}{\partial \overline{Z}}\right) = -\frac{\partial \overline{P}}{\partial \overline{Z}} + \frac{1}{\overline{R}}\frac{\partial}{\partial \overline{R}}\left(\overline{R}\bar{\bar{S}}_{\overline{RZ}}\right) + \frac{\partial \bar{\bar{S}}_{\overline{ZZ}}}{\partial \overline{Z}} + (\rho\beta)_{nf} g\left(\overline{T} - \overline{T_0}\right) + (\rho\beta)_{nf} g\left(\overline{C} - C_0\right). \tag{3}$$

The energy equation:

$$\left(\rho c_p\right)_{nf}\left(\frac{\partial \overline{T}}{\partial \overline{t}} + \overline{U}\frac{\partial \overline{T}}{\partial \overline{R}} + \overline{W}\frac{\partial \overline{T}}{\partial \overline{Z}}\right) = K_{nf}\left(\frac{1}{\overline{R}}\frac{\partial}{\partial \overline{R}}\left(\overline{R}\frac{\partial \overline{T}}{\partial \overline{R}}\right) + \frac{\partial^2 \overline{T}}{\partial \overline{Z^2}}\right) + Q_0. \tag{4}$$

The concentration equation:

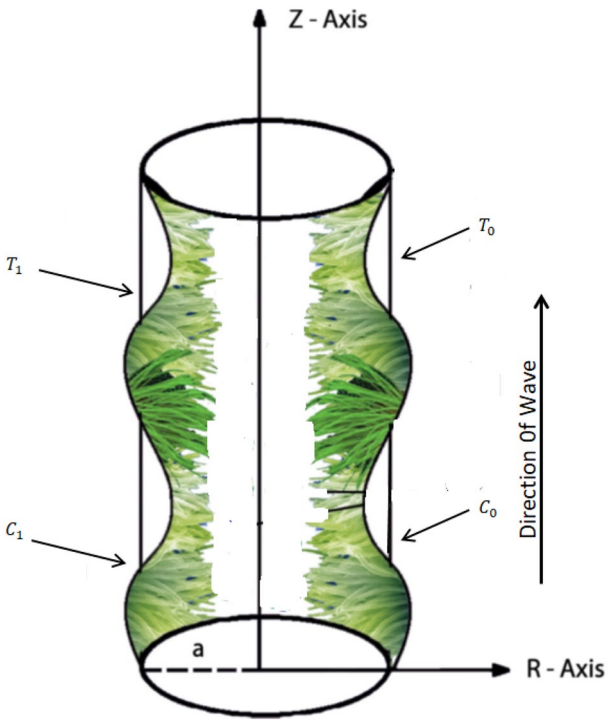

Figure 1. The schematic diagram of wall positions of tube when a peristaltic wave of slightly dilating amplitude propagates along it with velocity c.

$$\left(\frac{\partial \overline{C}}{\partial \overline{t}}+\overline{U}\frac{\partial \overline{C}}{\partial \overline{R}}+\overline{W}\frac{\partial \overline{C}}{\partial \overline{Z}}\right)=D_m\left(\frac{\partial^2 \overline{C}}{\partial \overline{R}^2}+\frac{1}{\overline{R}}\frac{\partial \overline{C}}{\partial \overline{R}}+\frac{\partial^2 \overline{C}}{\partial \overline{Z}^2}\right)+\frac{D_m K_T}{T_m}\left(\frac{\partial^2 \overline{T}}{\partial \overline{R}^2}+\frac{1}{\overline{R}}\frac{\partial \overline{T}}{\partial \overline{R}}+\frac{\partial^2 \overline{T}}{\partial \overline{Z}^2}\right). \tag{5}$$

The constitutive equation for the extra stress tensor $\overline{S}$ is defined as follows:

$$\overline{S}=\frac{\mu}{1+\lambda_1}\left(\dot{\overline{\gamma}}+\lambda_2\ddot{\overline{\gamma}}\right). \tag{6}$$

The flow is obtained by a sinusoidal wave train which move with a constant speed c along the wall of the tube, wall equation of the tube in the fixed system is given by:

$$\overline{R}=H\left(\overline{Z},t\right)=a+a\varepsilon\sin\frac{2\pi}{\lambda}\left(\overline{Z}-ct\right). \tag{7}$$

The equation of the cilia tips given mathematically in the form.

$$\overline{Z}=Z_0+\alpha\varepsilon a\sin\frac{2\pi}{\lambda}\left(\overline{Z}-ct\right). \tag{8}$$

The transformations between the two coordinate systems are:

$$\overline{r}=\overline{R},\overline{z}=\overline{Z}-ct,\overline{u}=\overline{U},\overline{w}=\overline{W}-c,\overline{p}=\overline{P}, \tag{9}$$

where $(\overline{u},\overline{w})$ and $(\overline{U},\overline{W})$ represent the velocity components of the moving and fixed frame.

The boundary conditions are given by

$$\frac{\partial \overline{W}}{\partial \overline{R}}=0,\frac{\partial \overline{T}}{\partial \overline{R}}=0,\frac{\partial \overline{C}}{\partial \overline{R}}=0,at\overline{R}=0$$

$$\overline{W}=\frac{-2\pi\varepsilon a\alpha c}{\lambda}\cos\frac{2\pi}{\lambda}\left(\overline{Z}-ct\right),\overline{T}=T_0,\overline{C}=C_0,at\overline{R}=H. \tag{10}$$

The thermo-physical properties can be written as:

$$\rho_{nf}=(1-\phi)\rho_f+\phi\rho_s,$$

$$(\rho\beta)_{nf}=(1-\phi)(\rho\beta)_f+\phi(\rho\beta)_s,$$

$$(\rho c_p)_{nf}=(1-\phi)(\rho c_p)_f+\phi(\rho c_p)_s,$$

$$\frac{K_{nf}}{K_f}=\frac{(K_s+2K_f)-2\phi(K_f-K_s)}{(K_s+2K_f)+\phi(K_f-K_s)}. \tag{10a}$$

The dimensionless parameter is given as follows:

$$\begin{aligned}&r=\frac{\overline{r}}{a},z=\frac{\overline{z}}{\lambda},u=\frac{\overline{u}}{c\delta},w=\frac{\overline{w}}{c},Re=\frac{\rho_f ac}{\mu_f},h=\frac{H}{a}=1+\varepsilon\cos2\pi z,S_{ij}=\frac{a}{\mu_f c}\overline{S}_{ij},p=\frac{a^2\overline{p}}{\mu_f c\lambda},\\&Q=\frac{Q_0a^2}{(T_1-T_0)K_f},\delta=\frac{a}{\lambda},t=\frac{c\overline{t}}{\lambda},\theta=\frac{\overline{T}-T_1}{T_1-T_0},\Theta=\ ,G_r=\frac{g\rho_f B_f a^2(T_1-T_0)}{c},Br=\frac{\rho g\alpha_c(-)}{c},\\&Sr=\frac{\rho_f D_m K_T(T_1-T_0)}{(C_1-C_0)},Sc=\frac{\mu_f}{D_m\rho_f}.\end{aligned} \tag{11}$$

Solution of the problem

In view of the above transformations (9) and non-dimensional variables (11), Eqs. (1, 2, 3, 4 and 5) are reduced to the following forms:

$$Re\delta^2\left(u\frac{\partial u}{\partial r}+(w+1)\frac{\partial u}{\partial z}\right)=-\frac{\partial p}{\partial r}+\delta\frac{1}{r}\frac{\partial}{\partial r}(rS_{rr})+\delta^2\frac{\partial S_{rz}}{\partial z}-\delta\frac{S_{\theta\theta}}{r}, \tag{12}$$

$$Re\delta\left(u\frac{\partial w}{\partial r}+(w+1)\frac{\partial w}{\partial z}\right)=-\frac{\partial p}{\partial z}+\frac{1}{r}\frac{\partial}{\partial r}(rS_{rz})+\delta\frac{\partial S_{zz}}{\partial z}+\frac{(\rho\beta)_{nf}}{(\rho\beta)_f}Gr\theta+\frac{(\rho\beta)_{nf}}{\rho\alpha_c}Br\Theta, \tag{13}$$

$$\left(\rho c_p\right)_{nf}ca\delta\left(u\frac{\partial\theta}{\partial r}+(w+1)\frac{\partial\theta}{\partial z}\right)=K_{nf}\left(\frac{1}{r}\frac{\partial}{\partial r}\left(r\frac{\partial\theta}{\partial r}\right)+\delta^2\frac{\partial^2\theta}{\partial z^2}\right)+QK_f, \tag{14}$$

$$Re\delta\left(u\frac{\partial\Theta}{\partial r}+(w+1)\frac{\partial\Theta}{\partial z}\right)=\frac{1}{Sc}\left(\frac{\partial^2\Theta}{\partial r^2}+\frac{1}{r}\frac{\partial\Theta}{\partial r}+\delta^2\frac{\partial^2\Theta}{\partial z^2}\right)+Sr\left(\frac{\partial^2\theta}{\partial r^2}+\frac{1}{r}\frac{\partial\theta}{\partial r}+\delta^2\frac{\partial^2\theta}{\partial z^2}\right). \tag{15}$$

and the boundary conditions in dimensionless form are:

$$\frac{\partial w}{\partial r}=0,\frac{\partial\theta}{\partial r}=0,\frac{\partial\Theta}{\partial r}=0,atr=0$$

$$w=-1,\theta=1,\Theta=1,atr=h. \tag{16}$$

Applying the approximation long—wavelength $\lambda >> 1$, small Renolds number $Re \ll 1$ and neglecting the wave number δ. Since Reynolds numbers are typically very low ($Re \ll 1$) in flow in small diameter tubules, analysis can be completed by approximating the inertia-free flow. Additionally, if the tube length is finite and equal to an integral number of wavelengths along with a constant pressure difference at the ends of the tube, the flow may be steady in the wave frame of reference. The governing Eqs. (12), (13), (14) and (15) in this situation, which make use of the long wavelength approximation, can be reduced to the following:

$$\frac{\partial p}{\partial r}=0, \tag{17}$$

$$-\frac{\partial p}{\partial z}+\frac{1}{r}\frac{\partial}{\partial r}(rS_{rz})+\frac{(\rho\beta)_{nf}}{(\rho\beta)_f}Gr\theta+\frac{(\rho\beta)_{nf}}{\rho\alpha_c}Br\Theta=0, \tag{18}$$

$$K_{nf}\left(\frac{1}{r}\frac{\partial}{\partial r}\left(r\frac{\partial\theta}{\partial r}\right)+\delta^2\frac{\partial^2\theta}{\partial z^2}\right)+QK_f=0, \tag{19}$$

$$\left(\frac{\partial^2\Theta}{\partial r^2}+\frac{1}{r}\frac{\partial\Theta}{\partial r}\right)+SrSc\left(\frac{\partial^2\theta}{\partial r^2}+\frac{1}{r}\frac{\partial\theta}{\partial r}\right)=0, \tag{20}$$

$$S_{rr}=\frac{2\delta}{1+\lambda_1}\left[1+\frac{\lambda_2c\delta}{a}\left(u\frac{\partial}{\partial r}+w\frac{\partial}{\partial z}\right)\right]\frac{\partial u}{\partial r},$$

$$S_{rz}=\frac{1}{1+\lambda_1}\left[1+\frac{\lambda_2c\delta}{a}\left(u\frac{\partial}{\partial r}+w\frac{\partial}{\partial z}\right)\right]\left(\frac{\partial w}{\partial r}+\delta^2\frac{\partial u}{\partial z}\right), \tag{21}$$

$$S_{zz}=\frac{2\delta}{1+\lambda_1}\left[1+\frac{\lambda_2c\delta}{a}\left(u\frac{\partial}{\partial r}+w\frac{\partial}{\partial z}\right)\right]\frac{\partial w}{\partial z},$$

$$S_{\theta\theta}=\frac{2\delta}{1+\lambda_1}\left[1+\frac{\lambda_2c\delta}{a}\left(u\frac{\partial}{\partial r}+w\frac{\partial}{\partial z}\right)\right]\frac{u}{r}.$$

The solutions of velocity, temperature and concentration with subject to boundary conditions (16) are given by

$$\theta=1+\frac{}{4K_{nf}}(h^2-r^2), \tag{22}$$

$$\Theta=1+\frac{SrSc}{4}\frac{}{K_{nf}}(r^2-h^2), \tag{23}$$

$$w=\frac{c_1r^4-4c_2Kr^2-4c_1h^2r^2-4c_2K\lambda_1r^2-4c_1h^2r^2\lambda_1+c_1\lambda_1r^2}{16K}+C_3, \tag{24}$$

The gradient of the pressure:

$$\frac{dp}{dz}=\frac{8c_1}{h^2(\lambda_1+1)}-\left[\frac{(\rho\beta)_{nf}Gr}{(\rho\beta)_f}+\frac{(\rho\beta)_{nf}Br}{\rho\alpha_c}\right]-\frac{5c_1h^2K}{6(\lambda_1+1)}+\frac{c_1K\lambda_1}{4(\lambda_1+1)}-\frac{c_1h^2K\lambda_1}{(\lambda_1+1)}-\frac{8F}{h^4(\lambda_1+1)}, \tag{25}$$

The volumetric flow rate:

$$F=\int_0^h wrdr. \tag{26}$$

The rise of pressure:

$$\Delta p_\lambda = \int_0^1 \frac{dp}{dz} dz. \tag{27}$$

The force of friction:

$$F_\lambda = \int_0^1 h^2 \left(-\frac{dp}{dz} \right) dz, \tag{28}$$

where

$$c_1 = \frac{(\rho\beta)_{nf} Gr}{(\rho\beta)_f} - SrSc \frac{(\rho\beta)_{nf} Br}{\rho\alpha_c}$$

$$c_2 = \frac{(\rho\beta)_{nf} Gr}{(\rho\beta)_f} + \frac{(\rho\beta)_{nf} Br}{\rho\alpha_c}, \tag{29}$$

$$C_3 = -1 + \frac{h^2 c_2 (1+\lambda_1)}{4} + \frac{c_1 Q h^2 (1+\lambda_1)}{4K} - \frac{c_1 Q h^4 (1+\lambda_1)}{16K}.$$

Results and discussion

This article discussed the Rabinowitsch Nanofluid of peristaltic flow with heat and mass transfer in a ciliated tube. The primary purpose of this section is to analyse the impact of pertinent parameters, including material parameters of Nanofluid, Nanofluid K_{nf}, thermal conductivity of fluid k_f, the viscosity at constant concentration α_c, thermal coefficient of nanofluid $(\rho\beta)_{nf}$ and heat source Q, on velocity (w), temperature (θ), concertation (C), pressure gradient $(\frac{dp}{dx})$, pressure rise (Δp_λ), friction force (F_λ) and shear stress (S_{rz}). Graphs are drawn to analyse the effects of the relevant parameter mentioned above using the MATLAB 2023a programming language. For this purpose Figs. (2, 3, 4, 5, 6, 7, 8 and 9) are sketched to measure the features of all parameters. In particular, the variations of parameters are examined.

We disclose the influence of various parameters on temperature and heat transfer mechanism. Figure 2 shows the effect of thermal conductivity of nanofluid K_{nf}, thermal conductivity of fluid k_f and heat source Q. It is clear from the Fig. 3 that temperature surges as we increase the value of parameter. This is because of the fact that $K_{nf} > 0$ indicates the heat generation. Which means temperature rises due to the internal friction of the nanofluid. elucidates the impact of convective heat transfer at the boundaries. It can be noticed from the temperature that for higher values of Q, temperature decreases. The reason behind this is the increased convective heat transfer at the boundaries which in turn results in decreased temperature, as well, we see an increasing manner in the temperature in the center of the tube. This result is in good agreement with the results obtained by Ellahi et al.[8].

Mass transfer cannot be ignored while dealing with heat transfer during multiple industrial and physiological fluid transport. Therefore, current subsection deals with the influence of different parameters on concentration profile. Figure 3 depicts the impact of thermal conductivity of nanofluid k_{nf}, thermal conductivity of fluid k_f and heat source Q on concentration C. Mass concentration decreases for enhancing the values of K_f, Q, while it increases with increasing of K_{nf}. Thus, increase in its value causes decrease in mass diffusion hence, resulting in mass accumulation. Thermal conductivity of nanofluid depicts the same behavior for increase in its concentration value. The behavior can be justified through the fact that increase in the value of K_{nf} results in large concentration gradient which in turn moves more mass. Thus, causing increase in mass concentration. All these concentration graphs reveal a parabolic graphical outcome and the concentration is minimum in the centre of tube while it enhances toward the tube walls. This is in good agreement with what was obtained in clinical practice because the nutrients diffuse out of the blood vessels to neighbouring tissues[32].

Figure 4 addresses the impact of related parameters on velocity profile w of Rabinowitsch nanofluid flow through ciliated tube. Figure 4 provides the graphical plot of velocity for thermal conductivity of nanofluid K_{nf}, coefficient of the viscosity at constant concentration α_c, thermal coefficient of nanofluid $(\rho\beta)_{nf}$ and heat source Q. The increasing K_{nf}, α_c reveal a decline in the velocity profile, while it increases with increasing $(\rho\beta)_{nf}$, Q. Since, the flow rate is directly related to velocity, therefore causing this upsurge in velocity for both types of fluids. In the culmination of above discussion we can say that velocity exhibits parabolic behavior for Dilatant fluid. The velocity profile outcomes depict that the flow has a maximum speed in the centre and it eventually decreases towards the tube walls. For more authenticity, this result is in good agreement with the results obtained by Rafiq et al.[32].

Figure 5 shows the axial pressure gradient expressed in terms of independent variable z is plotted for various corresponding parameters. Fluctuating behavior is shown by pressure gradient attaining its maximum at 0, 1, whereas approaching minimum at 0.5, while it disclose the graphical outcomes of pressure gradient $\frac{dp}{dz}$ for certain physical parameters. Figure 5 shows that $\frac{dp}{dz}$ increases for increasing value of heat source Q and Brinkman number Br, while it decline in the interval $[0, 0.2]$, as well, it increases in the interval $[0.2, 0.8]$, like that, it increases in the interval $[0.8, 1]$ for increasing values of Grashof number Gr and ratio of relaxation to retardation times λ_1. This shows the existence of high level flow through the tube without the need of greater pressure gradient. Figure is prepared to analyze the impact of Gr, Q, Br and λ_1 on $\frac{dp}{dz}$. It is clear from the Figure that pressure gradient simply decreases along the boundary of infinite tube. This result is in good agreement with the results obtained by Rafiq et al. et al.[32].

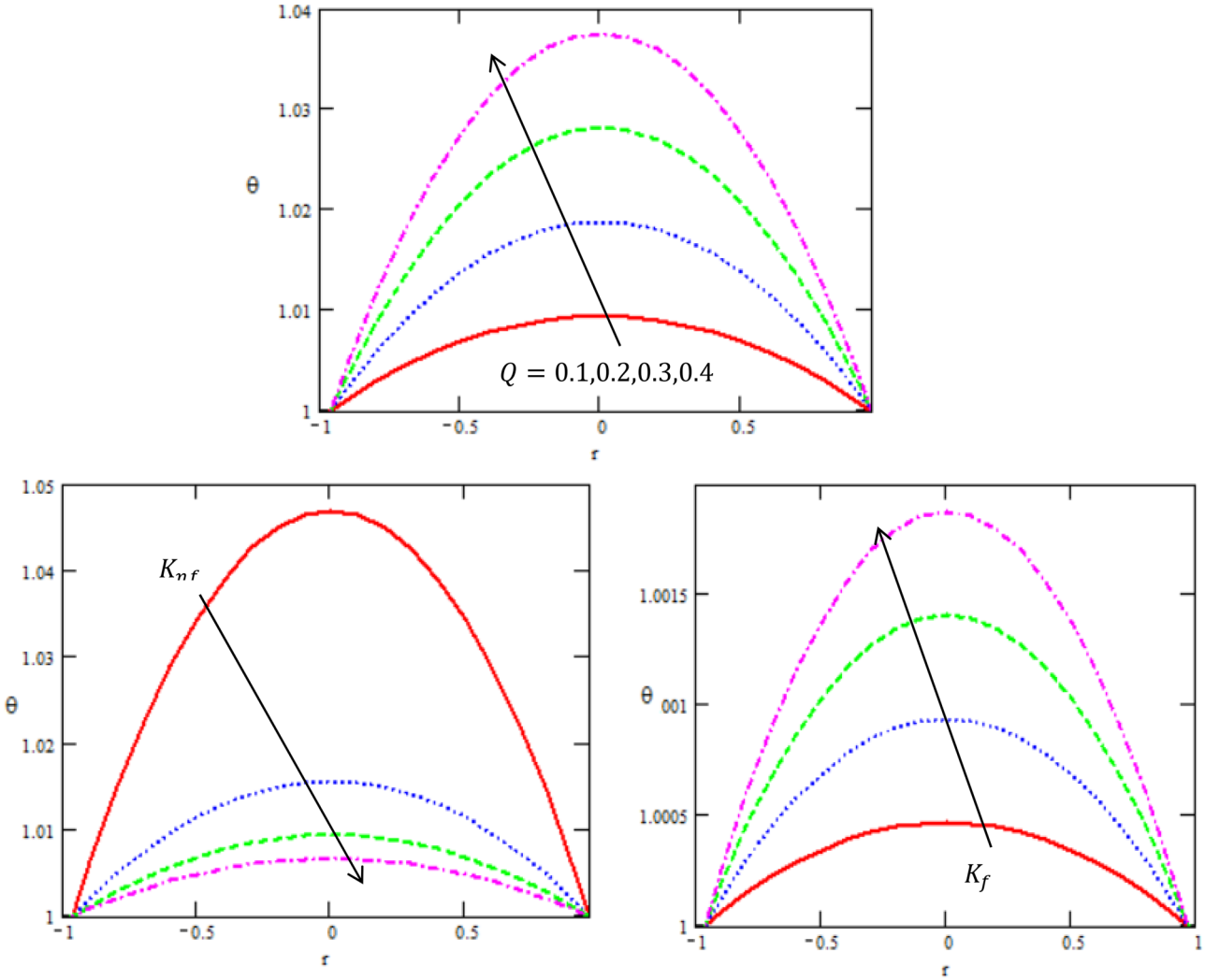

Figure 2. Variation between the temperature θ and the axial r with different values of Q, K_{nf}, K_f.

Figure 6 is developed to illustrate how embedding parameters correspond to pressure rise ΔP_λ per mean flow rate in this regard. Non-Newtonian fluid characteristics can easily be described by nonlinear nature of these curve. Figure 6 presents a graphical solution of ΔP_λ for increasing ratio of relaxation to retardation times λ_1, thermal coefficient of nanofluid $(\rho\beta)_{nf}$ and a decline in the value of ΔP_λ is observed in the region $\Delta P_\lambda \succ 0$ while it increases in the region $\Delta P_\lambda \prec 0$. It is observed that the graphical result of ΔP_λ for incrementing λ_1 and an increase in the value of ΔP_λ is noted in the region $\Delta P_\lambda \prec 0$ while it declines in the region $\Delta P_\lambda \succ 0$, while for increasing $(\rho\beta)_{nf}$ and an increase in the value of ΔP_λ in the regions $\Delta P_\lambda \prec 0, \Delta P_\lambda \succ 0$. Peristalsis, which occurred as a result of pressure difference, causes flow rate to be positive in the zone of peristaltic pumping, whereas peristalsis of the tube boundaries produces a free-pumping region. This result is in good agreement with the results obtained by Ellahi et al.[8].

Figure 7 indicate the disparities of the friction force F_λ on tube with regards to the rate of volume flow F for different values of the ratio of relaxation to retardation times λ_1, thermal coefficient of nanofluid $(\rho\beta)_{nf}$ in the peristaltic flow in a ciliated tube. In both figures, it is clear that the friction force in a ciliated tube has a non zero value only in a bounded region of space. It is observed that the friction force increases with increasing of ratio of relaxation to retardation times in the interval $[-300, 0]$, while it decreases in the interval $[0, 300]$, as well it decreases with increasing of the rate of thermal coefficient of nanofluid. On the other hand, these figures show that F_λ have an opposite behavior compared to the pressure rise Δp_λ versus the physical parameters.

Figure 8 displays the disparities of the value of axial tangential stress s_{rz} with regards to the $z-$ axis, which it has oscillatory behavior which may be due to peristalsis in the whole range of the z-axis for different values of the Brinkman number Br, heat source Q, The thermal expansion coefficient β_f and thermal conductivity of nanofluid K_{nf}. In both figures, it is clear that the value of tangential stress has a non zero value only in a bounded region of space. It is observed that the shear stress decreases with increasing of Br, Q, while it increases with increasing of β_f, K_{nf}. It is noticed that the variation in shear stress at the tube wall surface with and without nanoparticles in the fluid and varying values of the non-Newtonian fluid parameter. It is important to note that the shear stress at the tube wall exerted by the streaming flow carrying nanoparticles is higher in magnitude

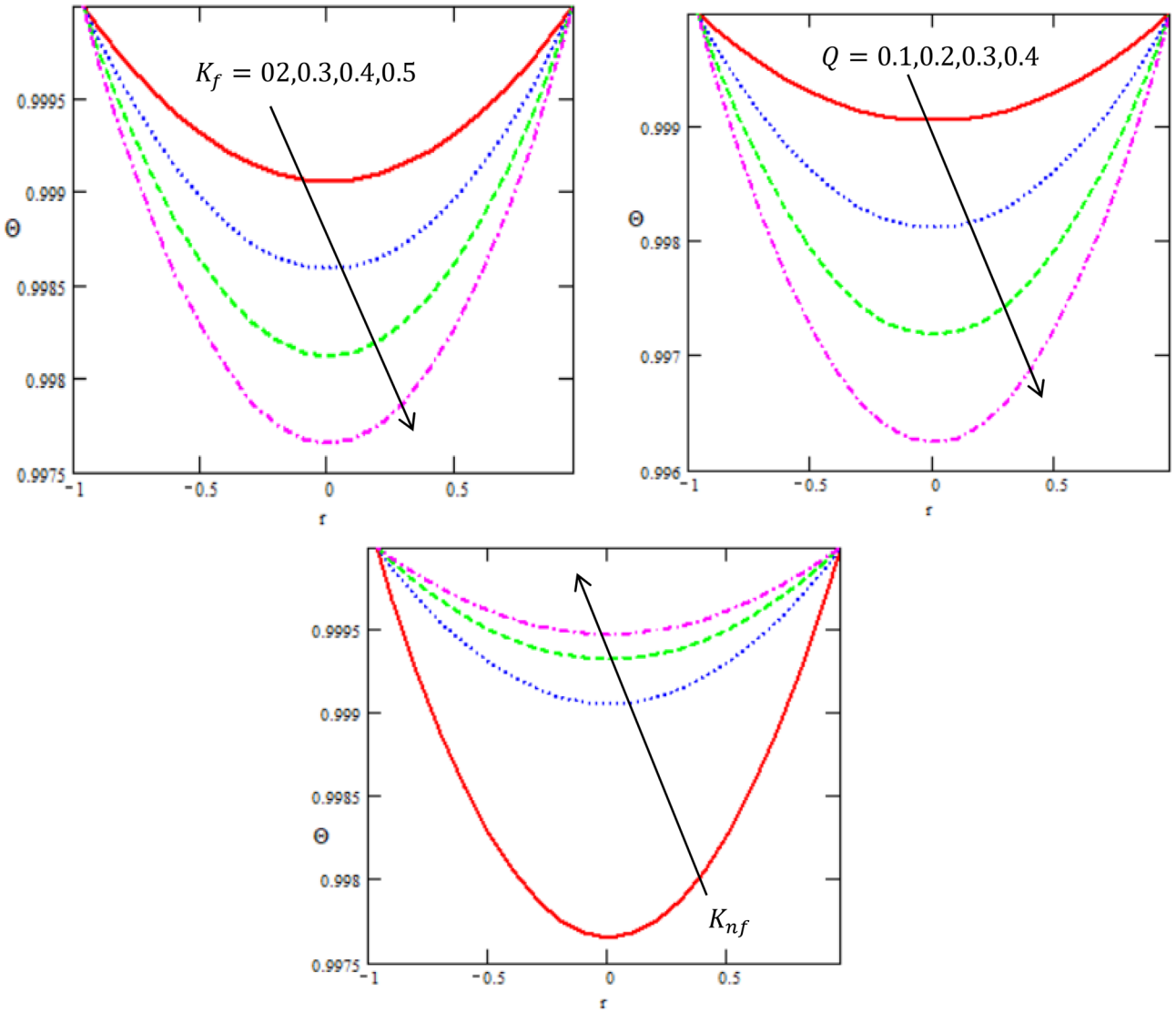

Figure 3. Variation between the concentration Θ and the axial-r with different values of Q, K_{nf}, K_f.

than that of fluid without nanoparticles. Moreover the values of shear stress are larger in case of a peristaltic fluid when compared with Newtonian fluid.

Figure 9 shows the 3*D* schematics concern the concentration Θ, axial velocity w and the axial pressure gradient $\frac{dp}{dz}$ with regards to r and z axes in the presence of heat source Q, the heat source Q, Grashof number Gr and the cilia length ε. It is observed that the concentration decreases with increasing Q, while it increasing with increasing of ε, axial velocity increases with increasing of Gr, while it decreases with increasing of ε, the pressure gradient increases with increasing of Gr. We obtain for all physical quantities, the peristaltic flow in 3D overlapping and damping when r and z increase to reach the state of particle equilibrium. The vertical distance has more significant of the curves were obtained, most physical fields are moving in peristaltic flow.

Conclusion

The Rabinowitsch nanofluid of peristaltic flow with heat and mass transfer in the ciliated tube is investigated. The present investigation utilized nanofluid model in a tube to analyse the peristaltic flow of non-Newtonian fluid in a ciliated tube with heat and mass transfer. A thorough understanding of peristaltic flow regulation and malfunction is possible by incorporating numerous effects that mirror natural events, especially in small arteries. These discoveries shed crucial new light on the properties of peristalsis during blood flow in human circulatory system. The knowledge gathered from this study could help diagnose and treat vascular diseases and promote scientific research. The following is a summary of the main conclusions drawn from the model:

1. Results obtained from the study indicate different flow behavior for the dilatant and nanofluid.
2. Thermal conductivity: This phenomenon causes the temperature to fall during peristalsis. This indicates that the nature of heat transfer within the system influences temperature fluctuations.

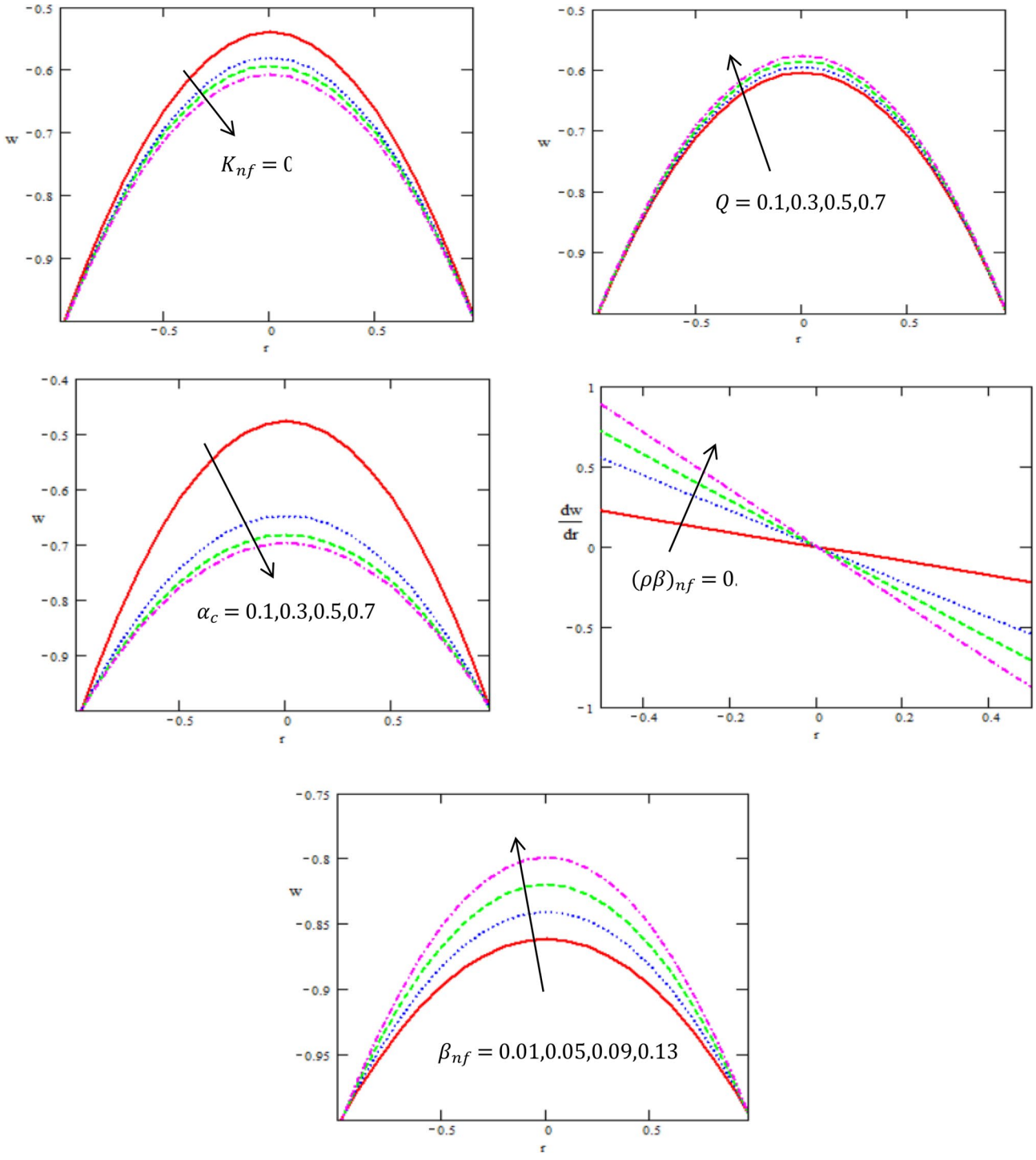

Figure 4. Variation between the velocity w and the axial-r with different values of $Q, K_{nf}\alpha_c, \beta_{nf}$.

3. Coefficient of the viscosity at constant concentration: The model shows that fluctuating viscosity raises both velocity and temperature during peristalsis. This suggests that viscosity impacts the temperature and flow dynamics of blood.
4. The graphical solutions of velocity depict that the flow has a maximum speed in the centre and it eventually decreases towards the duct walls.
5. The temperature graphs reveal a parabolic graphical outcome and increasing manner in the temperature in the center of the tube.
6. The concentration graphs reveal a parabolic graphical outcome and the concentration is minimum in the centre of duct whereas it enhances toward the duct walls.
7. The results presented in this paper should prove useful for researchers in science and engineering, as well as for those working on the development of fluid mechanics.

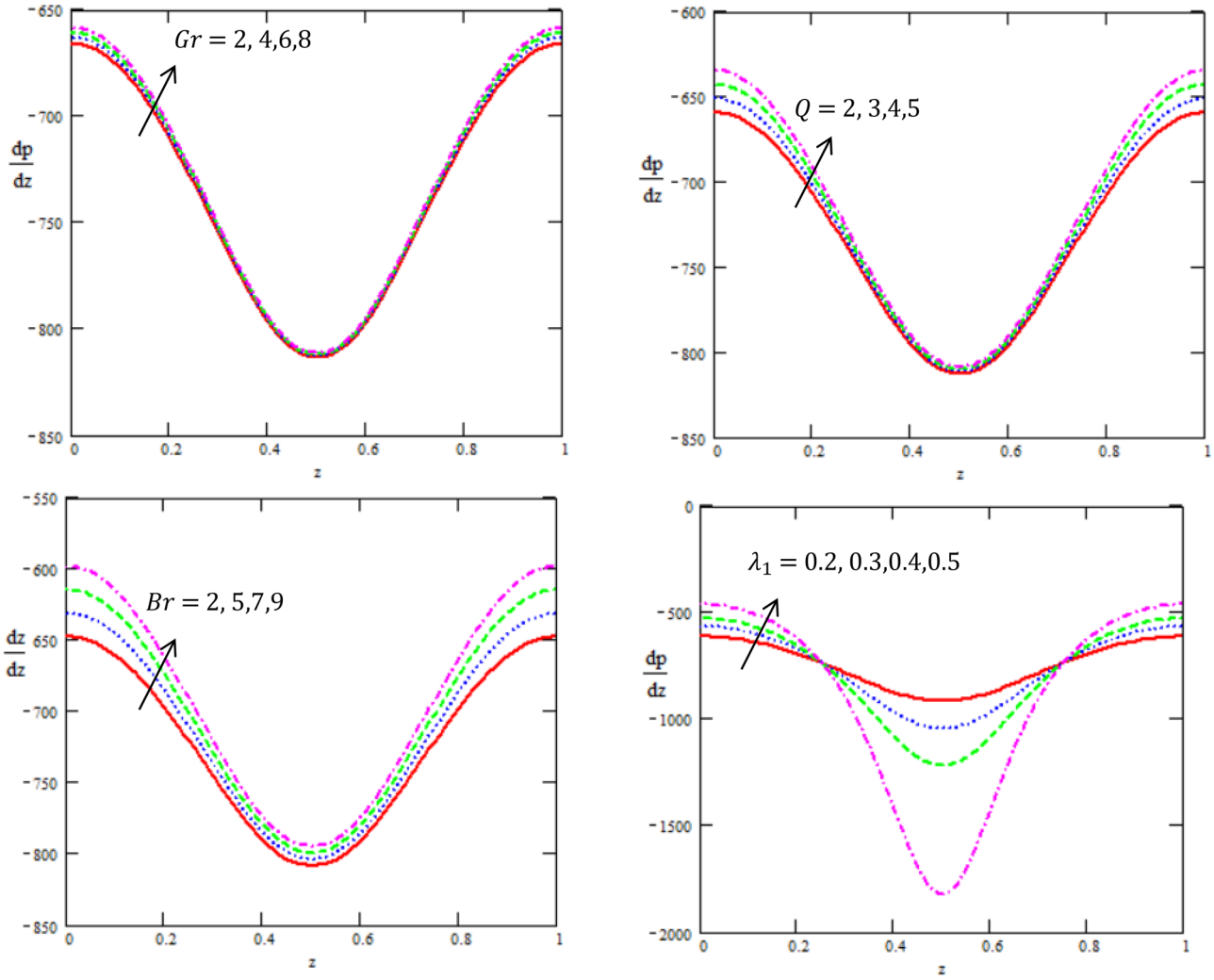

Figure 5. Variation between the gradient of pressure $\frac{dp}{dz}$ and the axial-z with different values of Gr, Q, Br, λ_1.

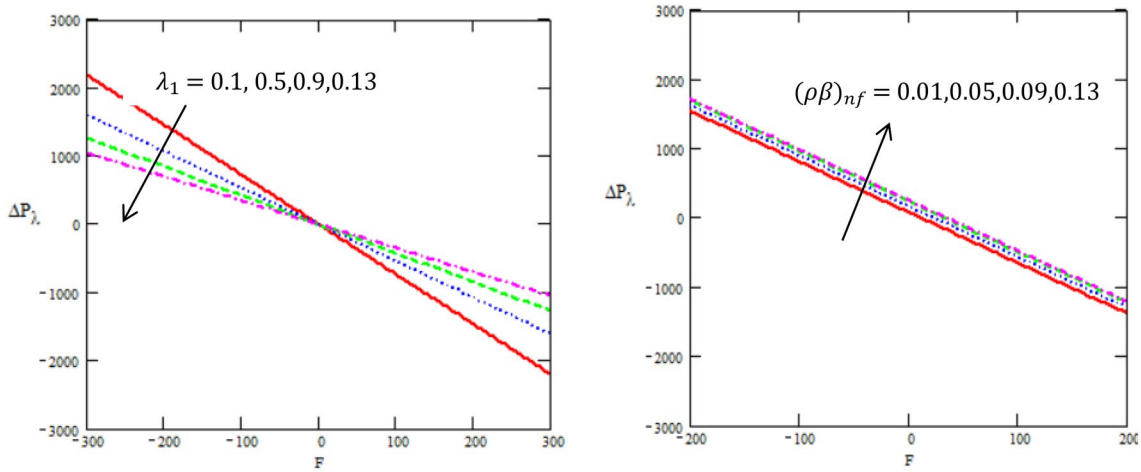

Figure 6. Variation between the rise of pressure Δp_λ and the axial-F with different values of λ_1, β_{nf}.

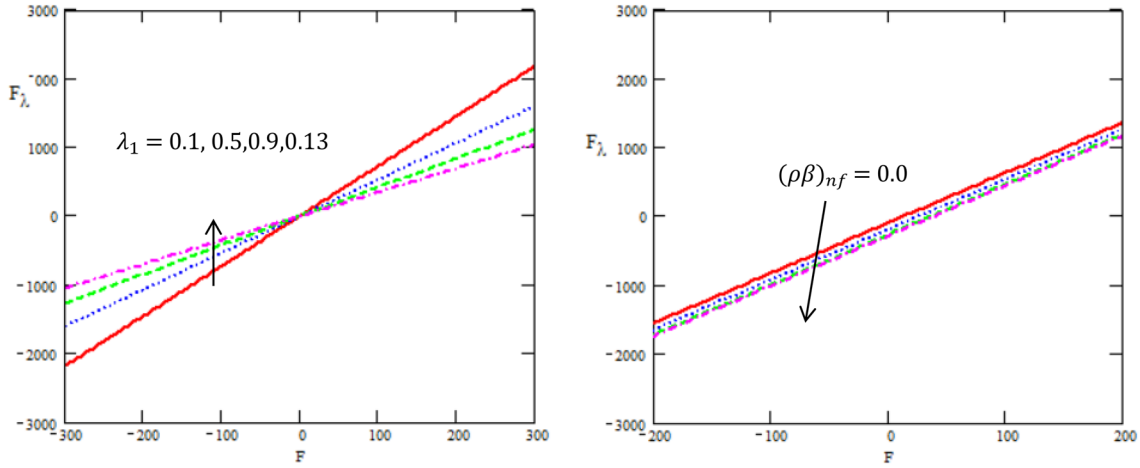

Figure 7. Variation between the force of friction F_λ and the axial-F with different values of λ_1, β_{nf}.

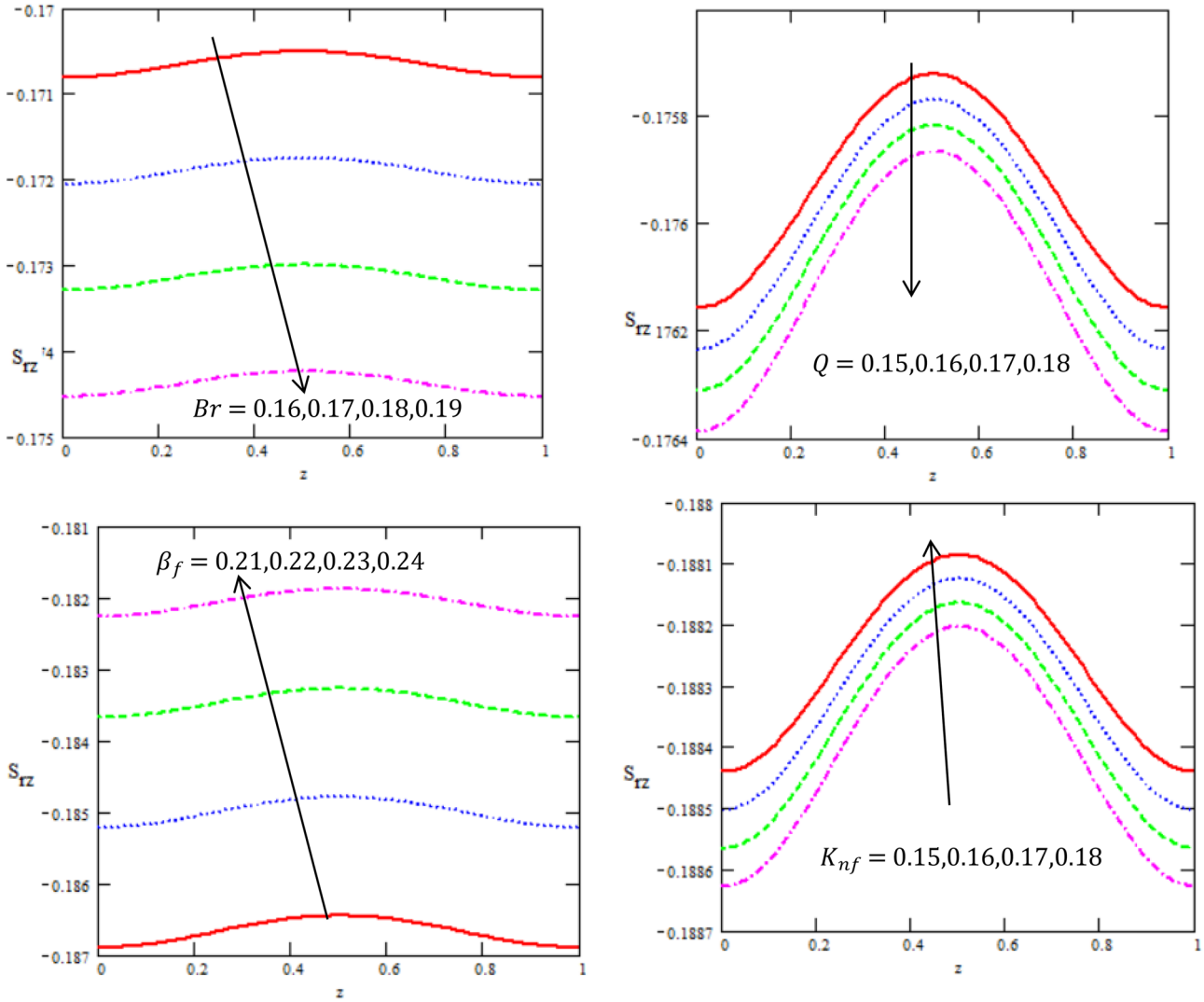

Figure 8. Variation between the shear stress S_{rz} and the axis-z with different values of Q, K_{nf}, β_f, Br.

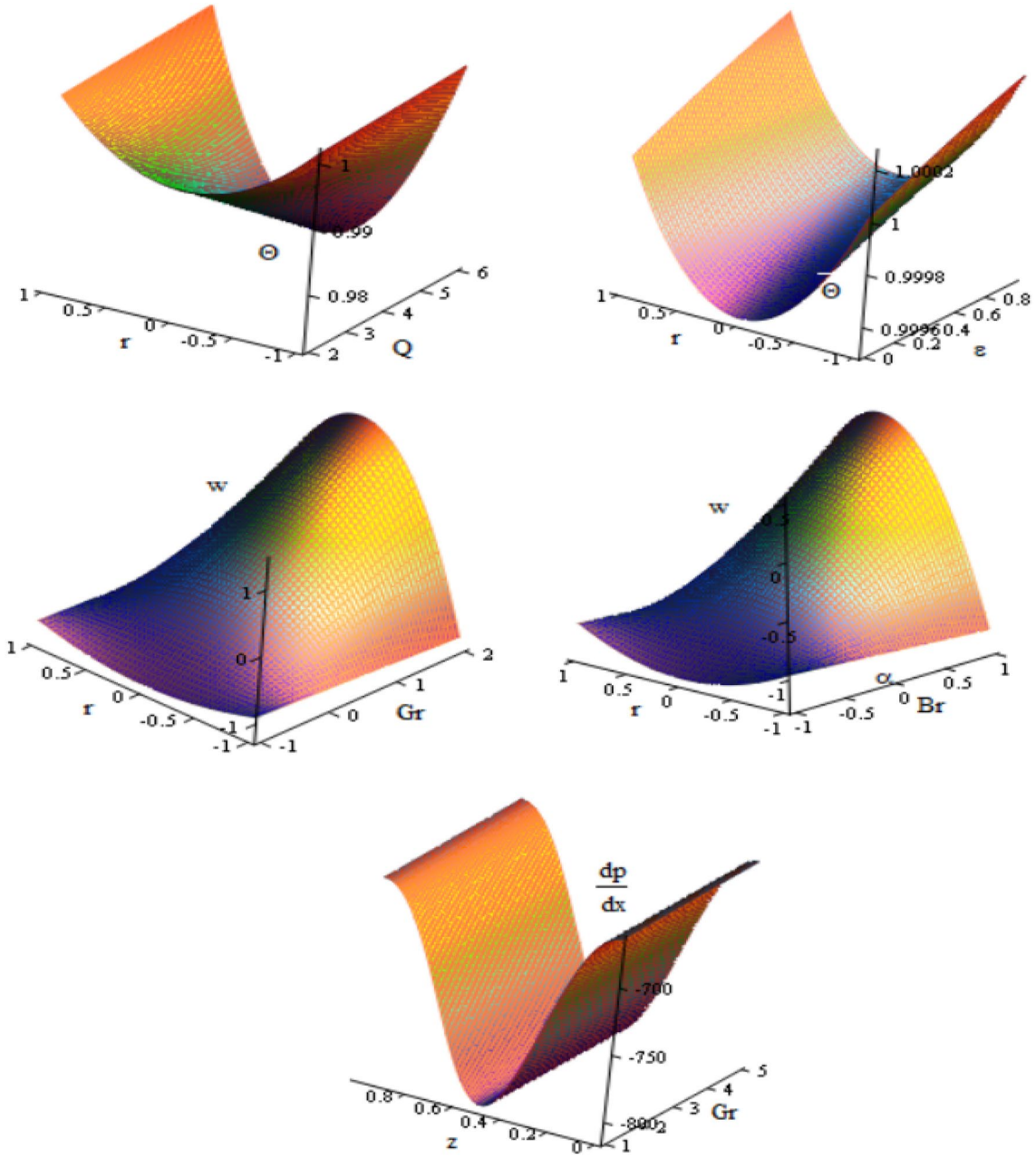

Figure 9. Discrepancies of the concentration Θ in 3D against r and z axis under the influence of Q, ε, velocity w under the influence of Gr, Br, pressure gradient $\frac{dp}{dx}$ under the influence of Gr.

Finally, one can concludes that the optimum state of the cases under consideration is applied various emerging parameters as affect the nanofluid properties within the tube because of its utilitarian aspects in dealing the peristaltic flow with heat and mass transfer.

Data availability

The datasets used and/or analyzed during the current study available from the corresponding author on reasonable request.

Received: 2 August 2023; Accepted: 18 September 2023
Published online: 25 September 2023

References

1. Akbar, N. S., Tripathi, D. & Bég, O. A. MHD convective heat transfer of nanofluids through a flexible tube with buoyancy: A study of nano-particle shape effects. *Adv. Powder Technol.* **28**, 453–462 (2017).
2. Narla, V. K., Tripathi, D. & Bég, O. A. Analysis of entropy generation in biomimetic electroosmotic nanofluid pumping through a curved channel with joule dissipation. *Therm. Sci. Eng. Progress* **15**, 100424 (2020).

3. Agoor, B. M., Ahmed, M. E. S. & Alam, H. The binary powell-eyring nanofluid of peristaltic flow with heat transfer in a ciliated tube. *Int. J. Fluid Mech. Therm. Sci.* **7**(1), 1–11 (2021).
4. Shit, G. C. & Sreeparna, M. Pulsatile flow of blood and heat transfer with variable viscosity under magnetic and vibration environment. *J. Magn. Magn. Mater.* **388**, 106–115 (2015).
5. Shit, G. C. & Sreeparna, M. Magnetic field interaction with blood flow and heat transfer through diseased artery having Abdominal Aortic Aneurysm. *Eur. J. Mech.-B/Fluids* **71**, 1–14 (2018).
6. Maqbool, K., Shaheen, S. & Siddiqui, A. M. Effect of nano-particles on MHD flow of tangent hyperbolic fluid in a ciliated tube: An application to fallopian tube. *Math. Biosci. Eng.* **16**(4), 2927–2941 (2019).
7. Tariqand, H. & Khan, A. A. Peristaltic transport of a second-grade dusty fluid in a tube. *J. Mech. Eng. Res.* **11**(2), 11–25 (2020).
8. Ellahi, R., Bhatti, M. M. & Vafai, K. Effects of heat and mass transfer on peristaltic flow in a non-uniform rectangular duct. *Int. J. Heat Mass Transf.* **71**, 706–719 (2014).
9. Nadeem, S., Riaz, A., Ellahi, R. & Akbar, N. S. Mathematical model for the peristaltic flow of nanofluid through eccentric tubes comprising porous medium. *Appl. Nanosci.* **4**, 733–743 (2014).
10. Shaheen, A. & Nadeem, S. Metachronal wave analysis for non-Newtonian fluid under thermophoresis and Brownian motion effects. *Results Phys.* **7**, 2950–2957 (2017).
11. Iqbal, J., Abbasi, F. M., Alkinidri, M. & Alahmadi, H. Heat and mass transfer analysis for MHD bio-convection peristaltic motion of Powell-Eyring nanofluid with variable thermal characteristics. *Case Stud. Therm. Eng.* **43**, 102692 (2023).
12. Abd-Alla, A. M., Abo-Dahab, S. M., Abdelhafez, M. A. & Thabet, E. N. Effects of heat transfer and the endoscope on Jeffrey fluid peristaltic flow in tubes. *Multidiscip. Model. Mater. Struct.* **17**(5), 895–914 (2021).
13. Akhtar, S., Almutairi, S. & Nadeem, S. Impact of heat and mass transfer on the Peristaltic flow of non-Newtonian Casson fluid inside an elliptic conduit: Exact solutions through novel technique. *Chin. J. Phys.* **78**, 194–206 (2022).
14. Mahmood, W., Sajid, M., Ali, N. & Sadiq, M. N. A new interfacial condition for the peristaltic flow of a micropolar fluid. *Ain Shams Eng. J.* **13**, 101744 (2022).
15. Tanveer, A., Khan, M., Salahuddin, T., Al Alwan, B. & Amari, A. Dynamics of Walters B fluid due to periodic wave in a convectively heated channel with internal heat generation. *J. Math. Comput. Simul.* **199**, 374–393 (2022).
16. Mansour, H. M. & Abou-zeid, M. Y. Heat and mass transfer effect on Non-Newtonian fluid flow in a non-uniform vertical tube with peristalsis. *J. Adv. Res. Fluid Mech. Therm. Sci.* **61**(1), 44–62 (2019).
17. Awan, S. E. *et al.* Numerical treatment for dynamics of second law analysis and magnetic induction effects on ciliary induced peristaltic transport of hybrid nanomaterial. *Front. Phys.* https://doi.org/10.3389/fphy.2021.631903 (2021).
18. Akbar, N. S. & Butt, A. W. Heat transfer analysis of Rabinowitsch fluid flow due to metachronal wave of cilia. *Results Phys.* **5**, 92–98 (2015).
19. Akram, S. *et al.* Impact of partial slip on double diffusion convection of Sisko nanofluids in asymmetric channel with peristaltic propulsion and inclined magnetic field. *Nanomaterials* **12**(16), 2736 (2022).
20. Akram, S., Athar, M., Saeed, Kh., Razia, A. & Muhammad, T. Hybridized consequence of thermal and concentration convection on peristaltic transport of magneto Powell-Eyring nanofluids in inclined asymmetric channel. *Math. Methods Appl. Sci.* **46**(10), 11462–11478 (2023).
21. Khan, Y. *et al.* The role of double-diffusion convection and induced magnetic field on peristaltic pumping of a Johnson-Segalman nanofluid in a non-uniform channel. *Nanomaterials* **12**(7), 1051 (2022).
22. Akram, S., Athar, M., Saeed, Kh., Imran, M. & Muhammad, T. Slip impact on double-diffusion convection of magneto-fourth-grade nanofluids with peristaltic propulsion through inclined asymmetric channel. *J. Therm. Anal. Calorim.* **147**, 8933–8946 (2022).
23. Khan, Y., Akram, S., Razia, A. & Al Sulaimani, H. Effects of double diffusive convection and inclined magnetic field on the peristaltic flow of fourth grade nanofluids in a non-uniform channel. *Nanomaterials* **12**(17), 3037 (2022).
24. Akram, S., Anjum, A., Khan, M. & Hussain, A. On Stokes' second problem for Burgers' fluid over a plane wall. *J. Appl. Comput. Mech.* **7**(3), 1514–1526 (2021).
25. Akram, S., Athar, M. & Saeed, Kh. Hybrid effects of thermal and concentration convection on peristaltic flow of fourth grade nanofluids in an Inclined tapered channel: Applications of double-diffusivity. *Case Stud. Therm. Eng.* **25**, 100965 (2021).
26. Farkhanda, S., Farkhanda, A. & Qamar, A. Impact of nanofluids and magnetic field on the peristaltic transport of a couple stress fluid in an asymmetric channel with different wave forms. *Therm. Sci.* **24**(2), 1407–1422 (2020).
27. Akram, S. *et al.* Convection theory on thermally radiative peristaltic flow of Prandtl tilted magneto nanofluid in an asymmetric channel with effects of partial slip and viscous dissipation. *Mater. Today* **35**, 106171 (2023).
28. Akram, S., Athar, M., Saeed, Kh., Razia, A. & Hussain, A. Influence of an induced magnetic field on double diffusion convection for peristaltic flow of thermally radiative Prandtl nanofluid in non-uniform channel. *Tribol. Int.* **187**, 108719 (2023).
29. Saeed, Kh., Akram, S. & Ahmad, A. Outcomes of partial slip on double-diffusive convection on peristaltic waves of Johnson-Segalman nanofluids under the impact of inclined magnetic field. *Arab. J. Sci. Eng.* https://doi.org/10.1007/s13369-023-07706-y (2023).
30. Khan, Y., Maria Athar, S., Akram, Kh., Saeed, A. R. & Alameer, A. Roll of partial slip on Ellis nanofluid in the proximity of double diffusion convection and tilted magnetic field: Application of Chyme movement. *Heliyon* **9**(4), e14760 (2023).
31. Akram, S., Athar, M., Saeed, Kh., Razia A. and Muhammad, T. Theoretical investigation of double diffusion convection of six constant Jeffreys nanofluid on waves of peristaltic with induced magnetic field: A bio-nano-engineering model. *Wave Random Complex Media.* https://doi.org/10.1080/17455030.2022.2134600 (2023).
32. Rafiq, M. *et al.* Impact of ciliated walls on peristaltic flow of Rabinowitsch fluid through flexible tube with heat/mass transfer. *Case Stud. Therm. Eng.* **45**, 102990 (2023).
33. Ahmed, R., Ali, N., Khan, S. U. & Tlili, I. Numerical simulations for mixed convective hydromagnetic peristaltic flow in a curved channel with joule heating features. *AIP Adv.* https://doi.org/10.1063/5.0010964 (2020).
34. Nadeem, S., Haider, J. A., Akhtar, S. & Mohamed, A. Insight into the dynamics of the Rabinowitsch fluid through an elliptic duct: Peristalsis analysis. *Front. Physiol.* **10**, 923269 (2022).
35. Abd-Alla, A. M., Abo-Dahab, S. M., Thabet, E. N., Bayones, F. S. & Abdelhafez, M. A. Heat and mass transfer in a peristaltic rotating frame Jeffrey fluid via porous medium with chemical reaction and wall properties. *Alex. Eng. J.* **66**, 405–420. https://doi.org/10.1016/j.aej.2022.11.016 (2023).
36. Abdelhafez, M. A., Abd-Alla, A. M., Abo-Dahab, S. M. & Elmhedy, Y. Infuence of an inclined magnetic feld and heat and mass transfer on the peristaltic fow of blood in an asymmetric channel. *Sci. Rep.* **13**, 5749. https://doi.org/10.1038/s41598-023-30378-5 (2023).
37. Abd-Alla, A. M., Abo-Dahab, S. M., Abdelhafez, M. A. & Thabet, E. N. Effects of heat transfer and the endoscope on Jeffrey fluid peristaltic flow in tubes. *Multidiscip. Model. Mater.* **17**(5), 895–914 (2021).
38. Abd-Alla, A. M., Abo-Dahab, S. M. & Alsharif, A. M. Peristaltic transport of a Jeffrey fluid under the effect of gravity field and rotation in an asymmetric channel with Magnetic field. *Multidiscip. Model. Mater.* **13**(4), 522–538 (2017).
39. Abd-Alla, A. M., Abo-Dahab, S. M. & Kilicman, A. Effect of radially varying MHD on the peristaltic flow in a tubes with an endoscope. *J. Magn. Magn. Mater.* **384**, 79–86 (2015).
40. Abd-Alla, A. M. & Abo-Dahab, S. M. Effect of rotation on peristaltic flow of fluid in a symmetric channel through a porous medium with magnetic field. *J. Comput. Theor. Nanosci.* **12**(6), 934–943 (2015).

Author contributions

A.M.A.-A. found a solution to the problem. S.D.A.D. created the numerical calculations, represented them graphically, and explained them physically. M.A.A. found a summary of the results and wrote the research. Y.E. developed the idea of research and the method of solution.

Funding

Open access funding provided by The Science, Technology & Innovation Funding Authority (STDF) in cooperation with The Egyptian Knowledge Bank (EKB).

Competing interests

The authors declare no competing interests.

Additional information

Correspondence and requests for materials should be addressed to Y.E.

Reprints and permissions information is available at www.nature.com/reprints.

Publisher's note Springer Nature remains neutral with regard to jurisdictional claims in published maps and institutional affiliations.